Critical stability of gold nanofingers on a zero-gradient stepped surface

2009 J. Phys.: Condens. Matter 21 445001

(http://iopscience.iop.org/0953-8984/21/44/445001)

J. Phys.: Condens. Matter **21** (2009) 445001 (6pp) doi:10.1088/0953-8984/21/44/445001

Critical stability of gold nanofingers on a zero-gradient stepped surface

F Yin, R E Palmer and Q Guo[1]

Nanoscale Physics Research Laboratory, School of Physics and Astronomy, University of Birmingham, Edgbaston, Birmingham B15 2TT, UK

E-mail: Q.Guo@bham.ac.uk

Received 17 April 2009, in final form 24 August 2009
Published 5 October 2009
Online at stacks.iop.org/JPhysCM/21/445001

Abstract

Numerous methods and techniques have been developed in recent years for the fabrication of two-dimensional and one-dimensional nanostructures that exhibit quantum effects. In order to understand the size-dependent stability of such structures, we have developed a method where the tip of the scanning tunnelling microscope (STM) is used to extract atoms from pre-fabricated gold nanofingers. The rate of atom removal as a function of the finger width at a constant temperature provides a direct evaluation of the size-dependent stability of the fingers. Our study reveals that the stability of the nanofinger has a strong dependence on the width of the finger.

(Some figures in this article are in colour only in the electronic version)

1. Introduction

The surface of a single crystal always consists of atomically flat terraces, as well as imperfections such as steps, adatoms, kinks and atomic vacancies [1, 2]. The concentration of adatoms and atomic vacancies on metal surfaces at room temperature is very low, ∼1 per billion for Cu and Ag for example [2], but the percentage of atoms at step edges is usually much higher, reaching ∼10% of the total number of surface atoms for some vicinal surfaces [2]. Because of the excessive free energy associated with a step, many important surface processes are controlled by step dynamics. For example, the step flow process in epitaxial growth [3] and step-induced formation of one-dimensional structures [4] depend strongly on the structure and stability of steps. A common approach for the study of step properties involves the exploitation of vicinal surfaces formed by cutting crystals with a small miscut angle with respect to a low-index plane [5]. A vicinal surface usually consists of a high density of steps arranged in a rather regular fashion, with the inter-step distance controlled mainly by the miscut angle if there is no step bunching. On a vicinal surface, all steps descend rather uniformly along a particular crystallographic direction. With face-centred-cubic (FCC) crystals, for instance, one can create a vicinal surface with step edges parallel to the close packed $[0\bar{1}1]$ direction and steps descending along the $[11\bar{2}]$ direction, see figures 1(a) and (b). In such a case, all steps are type B which is characterized by the (111) microfacet at each step edge [2]. However, if the steps are made to descend along the $[\bar{1}\bar{1}2]$ direction (opposite to the $[11\bar{2}]$ direction) then all the steps will be type A which is characterized by the (100) microfacet [2]. This difference in the structure of the two types of steps leads directly to different step energies and controls how the step edge interacts with atoms in the layer below [2]. On a vicinal surface as shown in figures 1(a) and (b), only one type of step is found on a chosen surface. In order to investigate how a type-A step interacts with a type-B step at nanometre distances, a unique zero-gradient stepped surface (ZGSS) [6, 8] has been successfully created on the (111) surface of gold.

A distinct feature of a ZGSS, as shown in figure 1(c), is that, in the direction perpendicular to the steps, an up step is always followed by a down step. Thus, there are equal numbers of up and down steps, making such a surface nominally flat, and hence the name 'zero gradient'. This kind of surface cannot be made using the same method used for creating a vicinal surface. So far it is only realized on the (111) surface of gold where atoms are extracted from a naturally existing step by the STM tip and are allowed to reassemble into rather regularly spaced narrow fingers [6–8]. The surface as illustrated in figure 1(c) differs from vicinal surfaces, not just in structural appearance, but more importantly in the energetics.

[1] Author to whom any correspondence should be addressed.

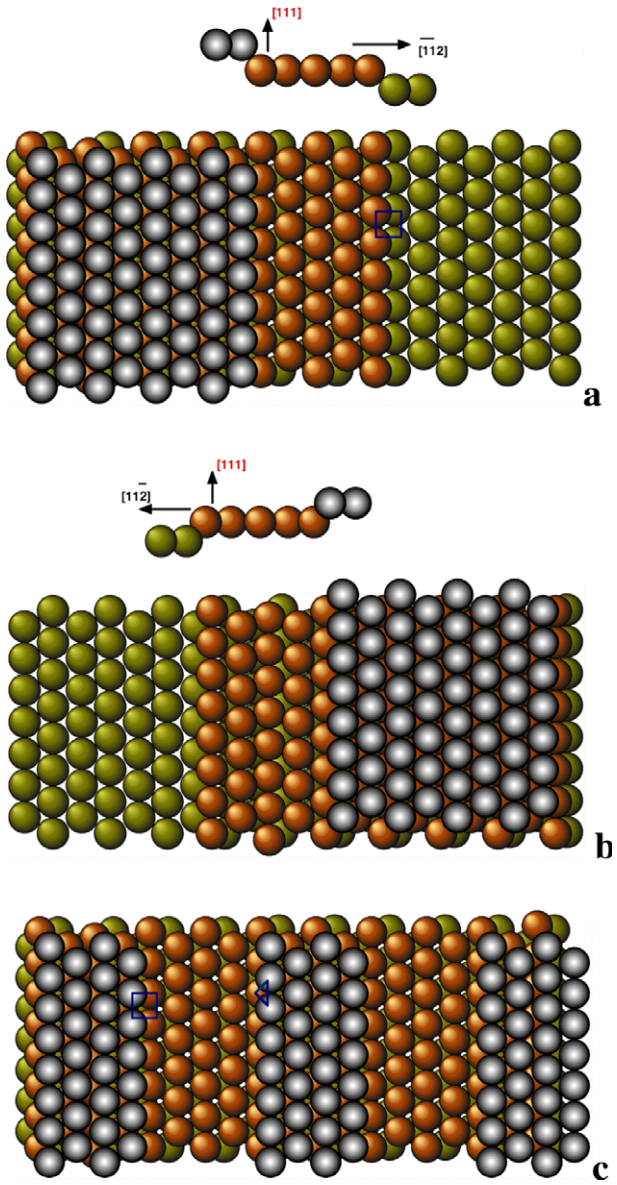

Figure 1. Ball models of surfaces vicinal to the (111) plane of a face-centred-cubic (FCC) crystal and a zero-gradient stepped surfaces. Different colours are used for atoms in different atomic layers. (a) Surface with steps down the [$\bar{1}\bar{1}$2] direction with a (100) microfacet at the step edge. (b) Surface with steps down the [11$\bar{2}$] direction with a (111) microfacet at the step edge. (c) A zero-gradient stepped surface. The top layer consists of parallel, narrow gold fingers one atomic layer in height. The blue triangle and the square illustrate the (100) and (111) microfacets, respectively.

For the vicinal surfaces shown in figures 1(a) and (b), the atomic structure of all steps on the same surface is intrinsically identical, and the step–step interaction arises between steps of the same type. For a ZGSS, adjacent steps are of different signs (+ for an up step and − for a down step). If the step energies for the up and down steps are different, which is true for the type-A and type-B steps on Au(111), one expects to observe many interesting phenomena on such a surface, such as the preferred attachment of atoms/molecules to one of the two adjacent step edges. Since the ZGSS consists of an array of aligned nanofingers, a thorough understanding of the atomic structure and stability of individual fingers becomes critically important in elucidating the physical properties of the surface as a whole.

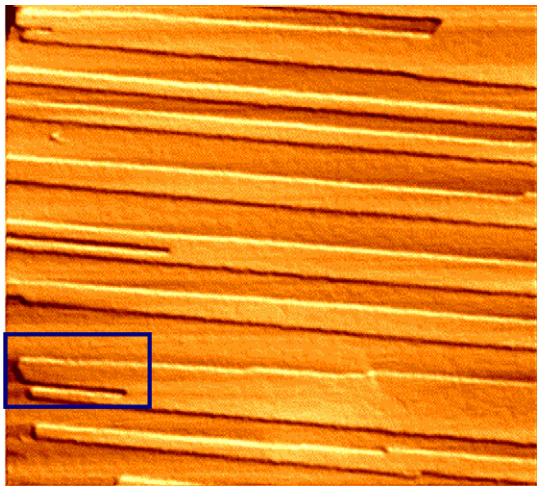

Figure 2. STM image (200 nm × 180 nm) of an array of parallel nanofingers on the Au(111) surface. The width of the fingers in this image ranges from 4 to 18 nm. The blue rectangle highlights an example of fingertip splitting.

2. Experiment

Experiments were conducted in an ultra-high vacuum (UHV) chamber with a base pressure of 2×10^{-10} mbar. STM imaging and surface modification were carried out using an Omicron VT-STM with electrochemically etched tungsten tips. The gold sample was prepared by thermal evaporation of gold onto a highly oriented pyrolytic graphite (HOPG) surface at 600 K, in a BOC Edwards evaporator, to form a gold film ∼500 nm thick. The sample was transferred to UHV and subjected to many cycles of Ar^+ sputtering and annealing at 900 K, until large terraces (a few hundred nm across) with the (111) orientation were identified in STM. Imaging was performed using a sample bias voltage ranging from 0.15 to 1.0 V and tunnelling currents of 50 pA–1 nA. We found that, under these 'low field' conditions, the surface was not modified by repeated scanning at either room temperature or 35 K. Modification of the fingers was performed using a voltage above 1.5 V and a current of 10–50 nA. These modification conditions are similar to those used for creating the fingers in the first instance [6, 8].

3. Results and discussion

Figure 2 shows an STM image of a typical ZGSS which consists of a number of parallel gold fingers of slightly different widths. It can be seen that these fingers are preferentially aligned in one direction. In fact, by examining a large number of STM images, we find that gold fingers on Au(111) can be made to point in any one of the three ⟨110⟩ directions such that the step edges consist of close packed atoms. Earlier observations of Wang and Moskovits [9] on Au(111) led to the incorrect conclusion that fingers point in

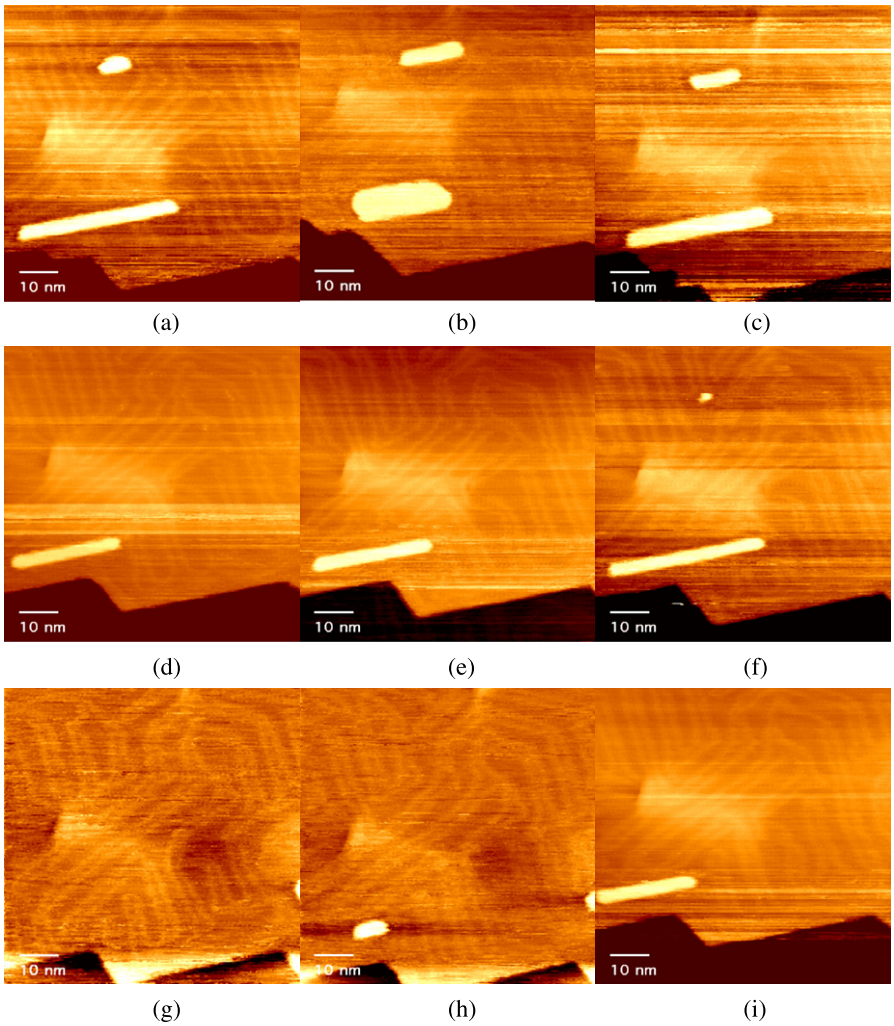

Figure 3. STM images (76 nm × 76 nm) showing the gradual change in the shape of a long, isolated finger caused by repeated scans of the STM tip with a bias voltage of 1.6 V and tunnelling current of 16 nA. The images were collected during the modification scans. From (a) to (d) the width of the finger decreases until the minimum width of 3.5 nm is reached in (d). Afterwards, the width of the finger remains constant whilst the length is reduced. The number of scans performed after collecting the initial image in (a) was: (b) 9; (c) 12; (d) 14; (e) 17; (f) 19; (g) 23; (h) 29; (i) 33.

the $[11\bar{2}]$ direction. We have performed numerous experiments with various scanning parameters including different scanning directions, and the fingers produced are always aligned with the $\langle 110 \rangle$ directions [6, 8], which is consistent with an independent study by Phark *et al* [10]. Splits at fingertips can be seen in figure 2. However, we find that splitting only occurs for fingers which are initially broader than ∼8 nm. This immediately points towards a width-dependent stability of the fingers. All the fingers are exactly one atomic layer high, but the width has a narrow but continuous distribution with an average value of around 5 nm. To study the width dependence of the finger stability, we fabricated two isolated fingers on a flat surface and observed how their width changed as atoms from the side of the fingers were removed by the STM tip. The isolated fingers were made following the same procedure as described previously [6] from an existing small gold island. The use of isolated fingers, rather than an array of fingers as shown in figure 3, is to eliminate atom transfer between neighbouring fingers. This way, the shape change of the individual fingers does not involve the complexity of atom exchange between different fingers. Information from such experiments on the property of isolated fingers is essential for studying the stability of an array of fingers and thus the stability of the surface as a whole. The level of mutual interaction between the nanofingers is expected to depend strongly on the nearest-neighbour distances, and this is a topic of ongoing research in our laboratory.

Figure 3 shows a sequence of STM images taken at room temperature in an area containing the two isolated, pre-fabricated fingers. As the STM tip repeatedly scans this area with 1.6 V bias voltage and 16 nA tunnelling current, the fingers get gradually modified. It needs to be pointed out that the observed changes to the fingers are exclusively initiated by the STM tip. Under more gentle scanning conditions with less than 50 pA current, no gross change to the fingers can be observed for hours. Because of the atomic scale changes to the STM tip from time to time, the bias voltage and the tunnelling current used to modify the fingers need to

be adjusted accordingly. The scan speed used for the images in figure 3 is 50 nm s^{-1}, although a typical scan speed ranges from 200 to 2000 nm s^{-1}. The smaller finger near the top of the image disappears after a short period of time, whilst the changes to the longer finger are continuously recorded (the apparent broadening of the smaller finger just before it disappears is likely caused by the tendency for the finger to change into a rounded shape to minimize the total step energy; this only occurs once the length becomes comparable to the minimum width). As can be seen in figure 3, the width of the long finger decreases from 8.4 nm, figure 3(a), to 3.5 nm, figure 3(d). The decrease of the finger width is accompanied by an increase in the finger length, confirming that atoms are removed from the two edges of the finger and are re-captured by the fingertip. Once the finger reaches 3.5 nm in width, it stops narrowing with further STM scanning and gradually becomes shorter as shown in figures 3(d)–(h). The shortening of the finger at a constant finger width shows that, under the experimental conditions applied, the STM tip is also capable of removing atoms from the fingertip. The increase in finger length as shown in figures 3(a)–(c) thus occurs because more atoms are transferred from the edges of the finger to the fingertip than are removed from the fingertip. Eventually, the finger disappears altogether, figure 3(i).

The nine images shown in figure 3 are a selection from a series of 38 images altogether collected from this modification run. For all the recorded images, we measured the width of the finger and plotted it as a function of the number of scans, figure 4. From this graph we see that, for fingers wider than ∼8 nm, approximately two rows of atoms are removed from the finger by each scan. It needs to be pointed out that one should not take it for granted that atoms are always moved from both steps with the same probability. The two steps have different local structures [6] and indeed it was shown previously that it is possible to induce faceting of the type-A step only [8]. In figure 3, there is a relatively long and straight atomic step near the bottom of each image. This step does not show gross changes during the whole process and is thus used as a reference point. When the distances from the two step edges of the finger to this reference step are measured, it is found that the upper step edge (the one that is furthest away from the reference point) moves closer to the reference step whilst the lower step moves away. Therefore atoms are lost from both step edges under the experimental conditions applied. As the finger becomes thinner, the reduction in width per scan is reduced as indicated by the change of curvature of the graph. This is obviously related to an increased stability of the gold finger as its width is reduced. The minimum width of a stable finger is observed to be 3.5 nm. Experiments have been performed on several gold fingers similar to that shown in figure 3, leading to the same findings, proving that the enhanced stability of the gold finger with reduced width is a rather universal phenomenon. When different bias voltages or different tips are used, the width of the finger can change at slightly different rates, but the final stable width is always 3.5 nm and the overall trend displayed in figure 4 is rather insensitive to the scanning parameters. The scan rate does not have an observable effect. As mentioned already, atoms are

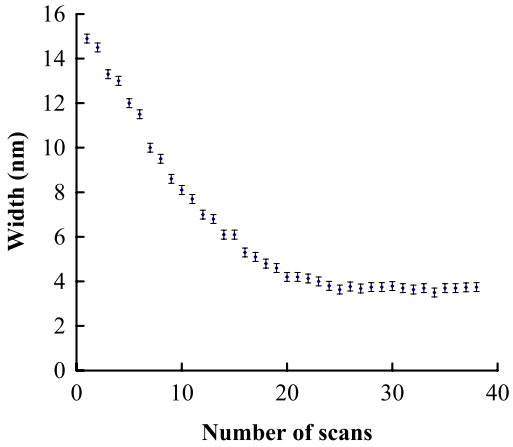

Figure 4. The width of a gold finger plotted against the number of modification scans with the STM tip.

removed by the STM tip from both the two parallel edges and the fingertip, thus the total number of atoms within the finger is not necessarily conserved because some atoms are moved by the STM tip to other parts of the surface. This can be clearly seen in figures 3(d) and (e), where once the supply of atoms from the edges ceases, the finger loses atoms and becomes shorter. From figures 3(a) to (d), the mass of the finger is more or less conserved. The finger as shown in figure 3 cannot be narrowed further using the experimental conditions applied to this experiment. If the electric field below the tip is increased to enhance the level of force acting on the surface atoms, further modification to the finger is possible. However, more aggressive scans would cut the finger into shorter segments instead of making the finger narrower. The overall result is that no fingers below 3.5 nm can be found on the surface, and the minimum stable finger on the surface has a width of 3.5 nm. Regarding the destiny of all the gold atoms from the two fingers in figure 3, we find that the atoms are re-deposited at nearby step edges. Growth at one of the step edges near the bottom of the image is clearly visible.

Figure 5 shows a schematic diagram illustrating the process of tip-induced narrowing of the gold finger. As the tip moves above a step edge, edge atoms are displaced away from the step by the localized electric field underneath the tip [6]. These atoms then diffuse and some of them are captured by the fingertip, leading to an increase in the finger length as demonstrated in figures 3(a)–(c). Although the data in figure 4 provide direct experimental evidence of an increased stability of the gold finger as its width is reduced, the reason for this increased stability is by no means obvious. The slope of the graph in figure 4 is nearly constant for a finger width above 8 nm, indicating a width-independent stability for wide fingers. This is more or less expected because each time a row of atoms is removed, the local structure of the new step edge is identical to that of the step edge before atom removal.

Provided that the two parallel steps of the finger do not interact with each other, the force required to remove atoms from the step edges should be independent of the finger width. Our experimental observations thus suggest an increasing level of step–step interaction with the reduced distance between the

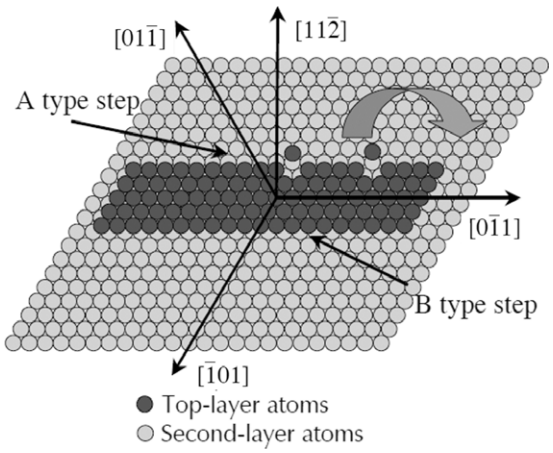

Figure 5. Schematic diagram illustrating the process of tip-induced atom transfer from the step edges to the fingertip. A few loose atoms near the upper step edge and in the vicinity of the fingertip are shown. The curved arrow indicates the process of atom transfer from the step edge to the fingertip.

steps. This interaction has the effect of stabilizing the step edges against modification. Therefore, when the step edges are far away from each other, they behave as non-interacting independent steps. Hence the removal of atoms from one step edge does not affect the atomic structure of the other step. This is the regime where the width of the finger decreases with nearly constant slope (figure 4). As the finger width is reduced, the step–step interaction grows in strength and it becomes more and more difficult to remove atoms from the steps. When the finger width approaches 3.5 nm, there are effectively only about 14 atoms between the two steps. (In such a case, if atoms were taken away from one of the steps, atoms on the other step would need to adjust their positions and vice versa.) There is thus a distance-dependent attractive interaction between the two steps.

The minimum width of the finger, 3.5 nm, observed at room temperature is a direct consequence of the competition between the step–step interaction, which stabilizes the narrower fingers against modification, and a destabilizing effect associated with the intrinsic surface reconstruction. At room temperature, the step–step interaction mentioned above is inevitably in competition with the herringbone reconstruction that always occurs on the (111) surface of gold. Considering a (111) surface of gold with the usual network of discommensuration lines. If we place a gold finger on top of this surface such that the finger is perpendicular to the discommensuration lines (i.e. in one of the allowed orientations for the finger), the atoms beneath the finger will resume their bulk positions because they are effectively second-layer atoms. Thus, for the layer of atoms that support this monolayer high gold finger, the original discommensuration lines are broken at the foot of each of the two step edges of the finger. Breaking the discommensuration lines costs energy, hence there is always the tendency for the broken lines to reconnect, and the only way for the lines to reconnect is to remove the finger on top. This serves as a destabilizing factor for the finger.

Under experimental conditions, as the finger gets thinner, there are thus two competing factors at play: (1) the step–step interaction which tends to stabilize narrow fingers and (2) the tendency for the reconnection of the discommensuration lines, acting against finger stability. At a critical width of 3.5 nm, the finger may disintegrate to allow the discommensuration lines from the two sides of the finger to connect. This process can take place only if the energy gained by joining up the discommensuration lines is more than the energy required to break the bonding of atoms within the finger. The energy required to break the atomic bonds within the finger scales more or less linearly with the finger width. The energy gained by rejoining the discommensuration lines is independent of the finger width, but scales with the length of the finger.

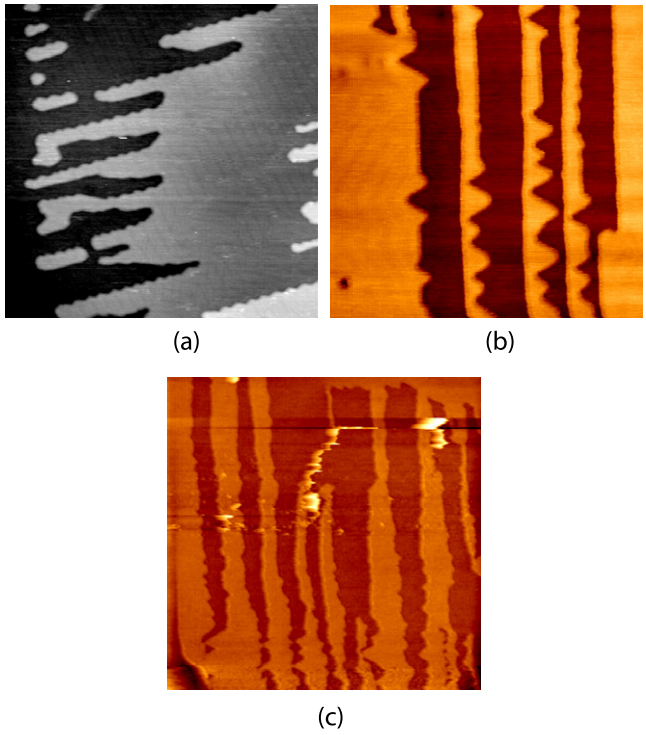

Figure 6. (a) STM image (175 nm × 175 nm) highlighting partial faceting of the gold fingers. This image is obtained after annealing the sample with pre-fabricated fingers to 330 K. Sample bias: 1.03 V; tunnelling current: 60 pA. (b) STM image (145 nm × 145 nm) showing the tip-induced faceting of the type-A step at room temperature. Bias voltage: 1.03 V, tunnelling current: 30 nA. The faster scan direction was perpendicular to the fingers. (c) STM image (215 nm × 215 nm) showing the changes to both type-A and type-B steps by the STM tip at 35 K. Bias voltage: 2.0 V, tunnelling current: 50 nA. Faster scan direction perpendicular to the fingers.

Finally, we would like to discuss the effect of temperature on the stability of the fingers. Raising the temperature of the sample to 330 K leads to one-sided (type-A step edge) faceting of the fingers as shown in figure 6(a). At room temperature, faceting is hindered and hence both edges of the finger are smooth. However, tip-induced faceting can take place if the scan direction is made perpendicular to the fingers, figure 6(b). It can be seen that tip-induced faceting at room temperature is more significant than thermally driven faceting at 330 K. As demonstrated previously, tip-induced faceting at room temperature leads to localized thinning of the finger, and when the narrowest part of the finger becomes less than 3.5 nm, the finger breaks [8]. Figure 6(c) shows

an STM image obtained at 35 K. At this low temperature, when the STM tip scans in the direction perpendicular to the fingers, both edges of the finger get modified. Due to insufficient thermal diffusion, the edges of the fingers have a jagged appearance. At room temperature, thermal diffusion ensures that each time a row of atoms is removed from the step edge, the two defect lines in the layer below the finger move closer to each other by one atom spacing. The transport of atoms to the tip of the finger is influenced by both thermal diffusion and tip-induced diffusion. The two contributions are not readily separable in the experiments performed to date, but temperature-dependent surface modification experiments with the STM tip are currently underway and the new experiments will help to resolve these issues.

4. Conclusion

In conclusion, we have demonstrated that the stability of the nanoscale fingers on the Au(111) surface at room temperature depends very strongly on the distance between the two opposite step edges. There exists a minimum width, ∼3.5 nm, for a stable finger at room temperature. The ZGSS surface provides a unique platform for the study of step–step interactions between two types of step edges separated by nanometre distances. In addition to the significant difference in the stability of the two types of steps, one also expects that the Ehrlich–Schwoebel barrier for atoms crossing a downwards atomic step [11, 12] having different heights at the two types of steps. This could lead to preferred attachment and growth at one of the two types of step edges when atoms or molecules are deposited onto the surface. This would result in an apparent one-way traffic for atoms and molecules on top of the finger and the realization of an atomic diode. The stacking faults on the normal, herringbone-reconstructed Au(111) surface have been widely used as nucleation sites for growing ordered nanoscale islands of other metals [13–15]. The new ZGSS surface will offer an extra dimension in controlling atomic movement on nanostructured surfaces.

Acknowledgment

This work was supported by the Engineering and Physical Sciences Research Council (EPSRC).

References

[1] Jeong H-C and Williams E D 1999 *Surf. Sci. Rep.* **34** 171
[2] Giesen M 2001 *Prog. Surf. Sci.* **68** 1
[3] Bartelt N C, Einstein T L and Williams E D 1992 *Surf. Sci.* **276** 308
[4] Gambardella P, Blanc M, Burgi L, Kuhnke K and Kern K 2000 *Surf. Sci.* **449** 93
[5] Kuhnke K and Kern K 2003 *J. Phys.: Condens. Matter* **15** S3311
[6] Guo Q, Yin F and Palmer R E 2005 *Small* **1** 76
[7] Guo Q, Yin F and Palmer R E 2006 *Phys. Rev.* B **73** 073405
[8] Yin F, Palmer R E and Guo Q 2006 *Surf. Sci.* **600** 1504
[9] Wang Z and Moskovits M 1992 *J. Appl. Phys.* **71** 75401
[10] Phark S H, Khim Z G and Yoon S 2007 *Curr. Appl. Phys.* **8** 822
[11] Ehrlich G and Hudda F 1966 *J. Chem. Phys.* **44** 1039
[12] Schwoebel R L and Shipsey E J 1966 *J. Appl. Phys.* **37** 3682
[13] Shiraka S, Fujisawa H, Nantoh M and Kawai M 2004 *Surf. Sci.* **552** 243
[14] Chambliss D D, Wilson R J and Chiang S 1991 *Phys. Rev. Lett.* **66** 1721
[15] Voigtlander B, Meyer G and Amer N M 1991 *Surf. Sci.* **255** L529